



Contribution of the two domains of *E. coli* 5'-nucleotidase to substrate specificity and catalysis



Ulrike Krug^a, Rica Patzschke^b, Matthias Zebisch^{a,c}, Jochen Balbach^b, Norbert Sträter^{a,*}

^aInstitute of Bioanalytical Chemistry, Center for Biotechnology and Biomedicine, University of Leipzig, 04103 Leipzig, Germany

^bInstitute for Physics, Martin-Luther-University Halle-Wittenberg, 06120 Halle/Saale, Germany

^cDivision of Structural Biology, Wellcome Trust Centre for Human Genetics, University of Oxford, Oxford OX3 7BN, UK

ARTICLE INFO

Article history:

Received 16 November 2012

Revised 21 December 2012

Accepted 2 January 2013

Available online 17 January 2013

Edited by Miguel De la Rosa

Keywords:

Enzyme kinetics

NMR

Phosphatase

Protein domain

Domain rotation

Protein evolution

ABSTRACT

***Escherichia coli* 5'-nucleotidase, a two-domain enzyme, dephosphorylates various nucleotides with comparable efficiency. We have expressed the two domains individually in *E. coli* and show by liquid state NMR that they are properly folded. Kinetic characterization reveals that the C-terminal domain, which contains the substrate-binding pocket, is completely inactive while the N-terminal domain with the two-metal-ion-center and the core catalytic residues exhibits significant activity, especially towards substrates with activated phosphate bonds (ATP, ADP, p-nitrophenyl phosphate). In contrast, residues of the C-terminal domain are required for efficient hydrolysis of AMP.**

© 2013 Federation of European Biochemical Societies. Published by Elsevier B.V. All rights reserved.

1. Introduction

Escherichia coli 5'-nucleotidase (5NT, E.C. 3.1.3.5) is a secreted periplasmic 60 kDa enzyme that hydrolyzes mono-, di- and trinucleotides, nucleotide sugars and bis(5'-nucleosidyl)polyphosphates [1,2]. The active site contains a dimetal center and resides at the interface of two domains (Fig. 1) [3,4]. The larger N-terminal domain (residues 26–342 of the mature protein) contains the active center with the catalytic Asp120-His117 dyad and two coordinated metal ions (Fig. 1B). The C-terminal domain consisting of residues 362–550 forms the substrate specificity pocket. The two domains are connected by a helix linker (residues 343–361, green in Fig. 1A) [3–5].

In a number of crystallographic studies various protein conformations of 5NT were observed differing in the relative orientation of the two domains [3,6–8]. Experiments to trap

the enzyme in the open and closed states indicate that this conformational change is crucial for the catalytic activity of the enzyme [6–8]. Most multi-domain enzymes open and close an interdomain cleft harboring the active site for a high catalytic efficiency [9]. The 5NT domain motion is unique because the large 96° domain rotation occurs around the center of the C-terminal domain. The interdomain cleft does not open but the active site residues slide along the interface [6]. While individual conformational states have been characterized in detail via X-ray crystal structures, information on the equilibrium and dynamics of the conformational switch is lacking. NMR spectroscopy is a powerful method to address these topics. However, signal assignment for a 60 kDa protein can be demanding but solved e.g., by the *divide and conquer* approach.

Here, we describe the expression and purification of the individual domains of 5NT. Via kinetic characterization we can quantitatively evaluate the contributions of the domains to substrate binding and catalysis in comparison to the full-length enzyme for the natural substrates ATP, ADP and AMP as well as the small artificial substrate p-nitrophenyl phosphate (pNPP). In addition, we show that NMR signal assignment of the individual domains will allow for future NMR analysis of the full-length enzyme.

Abbreviations: 5NT, *E. coli* 5'-nucleotidase; AMPCP, α,β -methylene-ADP; NDomN, terminal domain with residues 26–362 and a C-terminal hexahistidine tag; CDom, C-terminal domain with residues 363–550 and a C-terminal hexahistidine tag; pNPP, para-nitrophenyl phosphate; TROSY, transverse relaxation optimized spectroscopy

* Corresponding author. Address: Institute of Bioanalytical Chemistry, University of Leipzig, Deutscher Platz 5, 04103 Leipzig, Germany. Fax: +49 (0)341 9731319.

E-mail address: strater@bbz.uni-leipzig.de (N. Sträter).

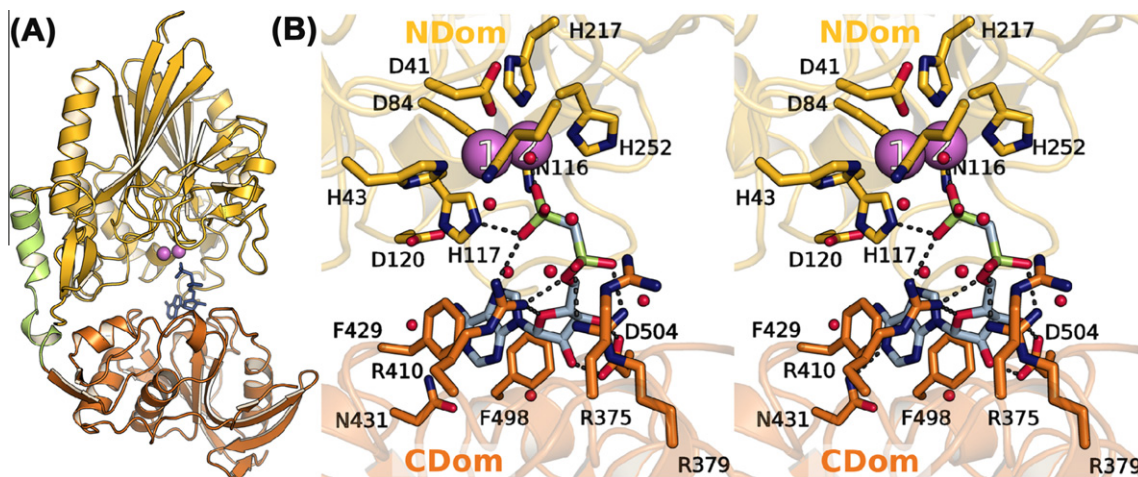


Fig. 1. Crystal structure of *E. coli* 5NT in the closed conformation (PDB:1HPU, chain C) [4]. (A) The N-terminal domain (residues 26–342) with two Mn^{2+} ions (pink) is colored in yellow, the helix linker (residues 343–362) in green and the C-terminal domain (residues 363–550) in orange. The ADP-analog AMPCP (blue) is located between the two domains. (B) Binding mode of AMPCP. The domains are colored as in A. Water molecules are shown as red spheres and interactions of the ligand with the protein as dashed lines.

2. Materials and methods

2.1. 5NT constructs

PCR-amplified genes encoding the two domains were cloned via *Nco*I and *Xho*I (Fermentas, St. Leon-Rot/Germany) sites in pET28a (Novagen, Madison, WI). All primers were ordered from biomers.net (Ulm/Germany). The gene of the 5NT N-terminal domain including the linker helix (in the following 5NT–NDom) was amplified using the primers 5′-CGATACACCATGGTAAAATTGCAGCGG GGCGTG-3′ and 5′-CGTATACTCGAGCACTTCCAGCTGCGCTTGGC-3′. After secretion into the periplasm and cleavage of the signal peptide the construct contained the mature amino acids Y26–V362 and had a molecular weight of 38.8 kDa. For cloning of the 5NT C-terminal domain (in the following 5NT–CDom) primers with the sequences 5′-CGATACACCATGGGCAAATAGGCGAAACC-3′ and 5′-CGTATACTCGAGCTGCCAGCTCACCTACC-3′ were used. The encoded construct of amino acids K363–Q550 had a molecular weight of 21.7 kDa, including an artificial methionine and a glycine at the N-terminus. No signal peptide was used for cytosolic expression of this domain, which lacks disulfide bridges.

The protein here referred to full-length 5NT consisted of residues Y26–Q550 [8]. All protein constructs contained an artificial leucine, glutamate and hexahistidine tag at the C-terminus.

2.2. Expression

All 5NT variants were expressed and purified using virtually identical protocols. *E. coli* BL21(DE3) cells harboring the respective expression plasmid were grown at 37 °C in LB medium with kanamycin (30 mg/l) to an OD_{600} of 0.5. Overexpression was induced by adding 1 mM isopropyl β -D-thiogalactopyranoside. Four hours after induction, cells were harvested by centrifugation and stored at –80 °C. ^{15}N -labeling for the NMR measurements was performed using modified M9 minimal medium containing 1 g/l $^{15}NH_4Cl$ (EURISO-TOP, Saarbrücken/Germany), 100 mg/l thiamin hydrochloride, 1 mM $MgSO_4$, 0.1 mM $CaCl_2$ and kanamycin. The expression in a ^{15}N background yielded 21 mg pure protein per 5 L culture medium for full-length 5NT, 11 mg per 5 L medium for 5NT–NDom and 28 mg per 1 L medium for 5NT–CDom.

2.3. Purification

10 g of cells were incubated for 30 min at 4 °C in 40 ml lysis buffer (500 mM NaCl, 25 mM imidazol, 100 mM Tris, pH 8) supplemented with 20 mg lysozyme (Merck, Darmstadt/Germany), 3 mM $MgCl_2$, 10 μ g/ml DNaseI and one tablet of cComplete, EDTA-free Inhibitor Protease Cocktail (both Roche, Mannheim/Germany). Cells were disrupted with a French Press and the solution was centrifuged. The supernatant was applied to a 5 ml HisTrap™ FF column, washed with lysis buffer and eluted with a linear gradient to 500 mM imidazole over 10 column volumes. Fractions were supplemented with 0.1 mM EDTA. Further purification steps were carried out as described before [8] using a 53 ml HiPrep 26/10 column in the desalting step, a MonoQ 10/100 GL column in anion exchange chromatography and a Superdex 200 16/60 in size exclusion chromatography. All columns were purchased from GE Healthcare. The protein was concentrated to 15 mg/ml and stored at –80 °C in size exclusion buffer (20 mM Tris, 50 mM KCl, 0.5 mM EDTA, pH 8.5). The protein concentration was determined spectrophotometrically at 280 nm.

2.4. Enzyme kinetics

The reaction buffer used for determination of the specific activity consisted of 20 mM BisTris (pH 7.0), 50 mM KCl and 20 mM $CaCl_2$. $CoCl_2$ was added to a concentration of 5 mM shortly before starting the reaction. The 5NT protein samples were diluted in reaction buffer supplemented with 50 μ g/ml BSA to prevent adhesion to the reaction tubes and with 5 mM $CoCl_2$. The reactions were started at room temperature by addition of 180 μ l of reaction buffer containing the respective concentration of substrate to 20 μ l of protein sample. Released phosphate was detected according to a modified malachite green assay [10,11]. The reaction was restricted to 10% phosphate release. After 20 min of color development the samples were measured at a Tecan-Sunrise Microplate Reader (Crailsheim/Germany) at a wavelength of 620 nm. Experimental data were fitted according to Michaelis–Menten using OriginPro 8G. It should be pointed out that the substrate concentrations used here were partly not sufficient to reach the saturation plateau. Due to an increased autohydrolysis of the substrates it was

not possible to use higher substrate concentrations in the malachite green assay. With the assumption that the AMP concentration was much smaller than the K_m -value the specificity constant of 5NT–NDom with AMP was calculated from the slope of the curve shown in Fig. 4B.

2.5. NMR experiments

In preparation for the NMR experiments samples were dialyzed three times against the 100-fold sample volume of 50 mM sodium phosphate buffer (pH 7.0). After addition of 10% D₂O ¹H/¹⁵N-TROSY-HSQC spectra were acquired with a Bruker Avance III 800-MHz spectrometer equipped with a cryogenic triple resonance at 308 K. The protein concentrations in the NMR experiments to record the spectra were 0.6 mM for full-length 5NT, 0.5 mM for 5NT–NDom and 0.7 mM for 5NT–CDom. Spectra, typically recorded for 2.5 h, were processed using NMRpipe [12] and analyzed using NMRview [13]. A spectrum of full-length 5NT in presence of a substrate analog was recorded after addition of 2.4 mM AMPCP (Sigma Aldrich, Germany).

3. Results

3.1. 5NT domains fold independently

Based on the known crystal structures [3,4,8] the N- and C-terminal domains of *E. coli* 5NT divided at positions 342–343 were cloned and expressed individually. To verify the structural integrity of both domains on a residue level NMR spectroscopy was employed. Full-length 5NT and both domains showed well dispersed ¹H/¹⁵N-correlation spectra indicating properly folded proteins (Fig. 2). Moreover, the superposition of spectra of the individual domains (Fig. 2A and B) and full-length 5NT clearly illustrates, that the majority of NMR resonances show very similar chemical shifts. Therefore, the overall fold of the domains remains intact upon separate expression.

It was crucial to express the 5NT–NDom construct with the linker helix (residues 343–361). A variant lacking this part of the structure results in a ¹H/¹⁵N-TROSY-HSQC spectrum with typical characteristics of a protein only partially structured (Fig. 2D). Besides some cross signals with good dispersion most of the signals

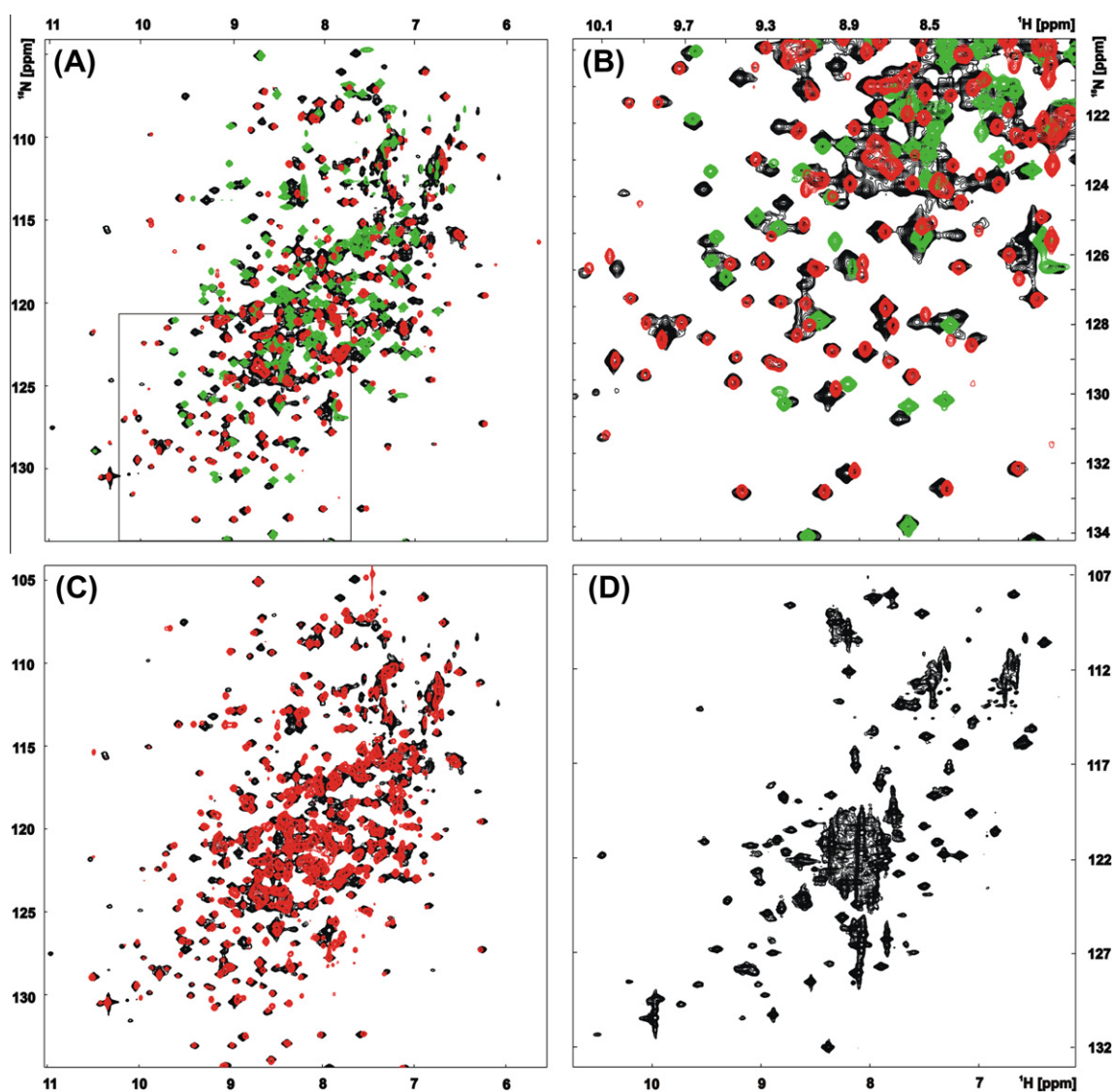


Fig. 2. ¹H/¹⁵N-TROSY-HSQC NMR spectra of *E. coli* 5NT variants. (A) The spectra of 5NT–NDom (red) and 5NT–CDom (green) are superimposed on the spectrum of full-length 5NT (black). In (B) a section (indicated by the box in A) of the superposition of spectra of all three proteins is depicted. (C) Superimposition of full-length 5NT in the absence of AMPCP (black) and in the presence of a fourfold excess of AMPCP (red). The spectrum for 5NT–NDom lacking the linker helix (residues 343–362) is shown in (D).

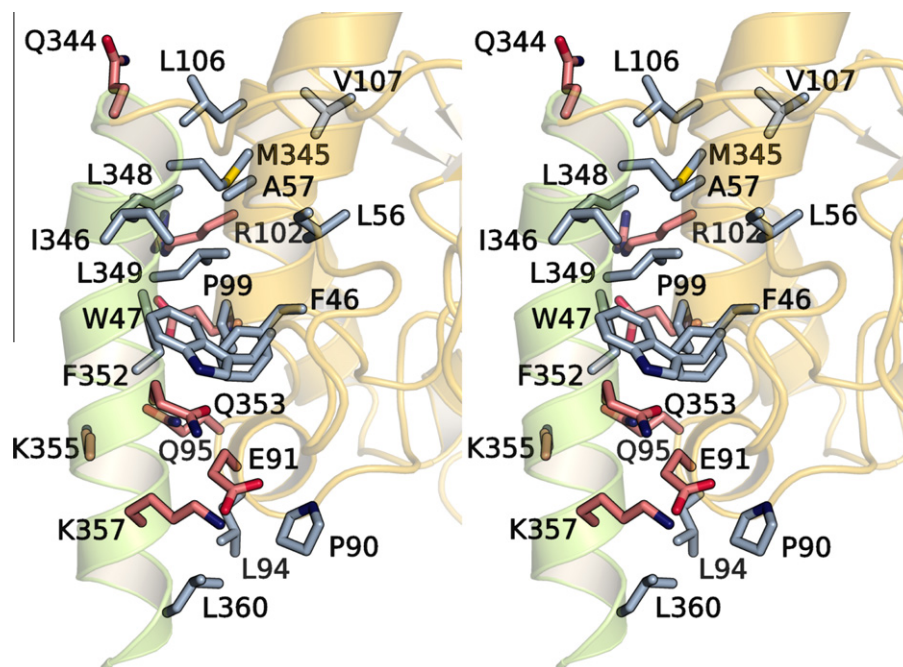


Fig. 3. Interactions between the *E. coli* 5NT N-terminal domain (yellow) and the helix linker (green). Residues with hydrophobic and polar interactions are colored in gray and red, respectively.

coincide in a spectral region of 8.3–9.3 ppm, which is indicative for unfolded or aggregated protein. An explanation for this behaviour is found upon close inspection of the interactions between the helix linker and the core of the N-terminal domain (residue 345–360) which are dominated by hydrophobic interactions (Fig. 3). The removal of the linker helix leads to exposure of this hydrophobic patch and possibly results in misfolding of 5NT–NDom. This also accounts for the observed reduction of activity of about 80% when 5NT–NDom was expressed without the helix linker (data not shown).

The $^1\text{H}/^{15}\text{N}$ -TROSY-HSQC spectrum of full-length 5NT shows relatively sharp and well separated signals for a 60 kDa protein (Fig. 2). This indicates a non-concerted, largely independent motion of both domains in the full-length protein. This motion gets not significantly affected upon binding of the non-hydrolyzable ADP-analog AMPCP on the chemical shift time scale of full-length 5NT. The addition of a fourfold excess of AMPCP gave correlation spectra of the same quality in respect to line width dispersion (Fig. 2C). The majority of cross peaks do not change chemical shift position. Several residues experience chemical shift changes indicating AMPCP binding.

3.2. Only the N-terminal domain has intrinsic catalytic activity

The enzymatic turnover and the kinetic parameters of full-length 5NT, 5NT–NDom and 5NT–CDom for the hydrolysis of ATP, ADP, AMP and pNPP were determined in the presence of Co^{2+} and Ca^{2+} (Fig. 4, Table 1). After purification in the presence of EDTA, the enzyme contains no bound metal ions, as indicated by crystal structures in the absence of added divalent metal ions (data not shown). Combination of Co^{2+} and Ca^{2+} ions were described to maximally activate the full-length enzyme and it is thus likely that the dimetal center is occupied by one Co^{2+} and one Ca^{2+} in the enzymatic tests carried out here [1].

3.2.1. Substrate specificity of full-length 5NT

E. coli 5NT hydrolyzes all three nucleotides with high efficiency and shows a preference for AMP and ATP over ADP. The catalytic

Table 1

Kinetic parameters of full-length 5NT and 5NT–NDom determined at room temperature for hydrolysis of AMP, ADP, ATP and pNPP in presence of 5 mM CoCl_2 and 20 mM CaCl_2 .

	k_{cat} (s^{-1})	K_{m} (μM)	$k_{\text{cat}}/K_{\text{m}}$ ($\text{M}^{-1} \text{s}^{-1}$)
<i>Full-length 5NT</i>			
AMP	459.1 ± 4.5	12.91 ± 0.85	$(3.56 \pm 0.24) \times 10^7$
ADP	613.2 ± 5.4	54.7 ± 2.4	$(1.122 \pm 0.051) \times 10^7$
ATP	757 ± 16	20.9 ± 2.8	$(3.62 \pm 0.49) \times 10^7$
pNPP	40.8 ± 2.9	5713 ± 783	$(7.1 \pm 1.1) \times 10^3$
<i>5NT–NDom</i>			
AMP	n.d.	n.d.	$(2.89 \pm 0.13) \times 10^{-1,a}$
ADP	45.6 ± 6.7	10151 ± 2107	$(4.5 \pm 1.1) \times 10^3$
ATP	36.5 ± 5.1	6807 ± 1499	$(5.4 \pm 1.4) \times 10^3$
pNPP	129 ± 26	21173 ± 5761	$(6.1 \pm 2.1) \times 10^3$

^a Calculated from the slope of the curve in Fig. 4B.

efficiency ($k_{\text{cat}}/K_{\text{m}}$) is more than 1000-fold higher towards the nucleotides compared to pNPP (Table 1). Most likely, the small substrate pNPP is not able to bind to the substrate binding pocket and thus forms no specific interactions with the protein in addition to the interactions of the phosphate group [7]. K_{m} and k_{cat} for the hydrolysis of pNPP determined here are in good agreement with previous data [7]. The K_{m} values of 12.9 μM determined for AMP and 20.9 μM for ATP are lower than the previously determined values of 33 μM [1], 45 μM [2], 74 μM [7] and 93 μM [14] for AMP and 120 μM [1] for ATP. These differences might be caused by different protein constructs, protein preparations, buffers, metal ion compositions and pH-values used in the various studies. Furthermore, substrate inhibition by AMP, ADP or ATP as described before [2,7,15] was not observed in our assays (Fig. 4). Since very similar buffer conditions have been used in the previous studies, the cause of this difference remains unclear. One possibility is that contaminations of inhibitory metal ions (present in the substrate stock solution) caused the inhibition at high substrate concentrations.

To the best of our knowledge, catalytic parameters for the hydrolysis of ADP by *E. coli* 5NT have not been described before.

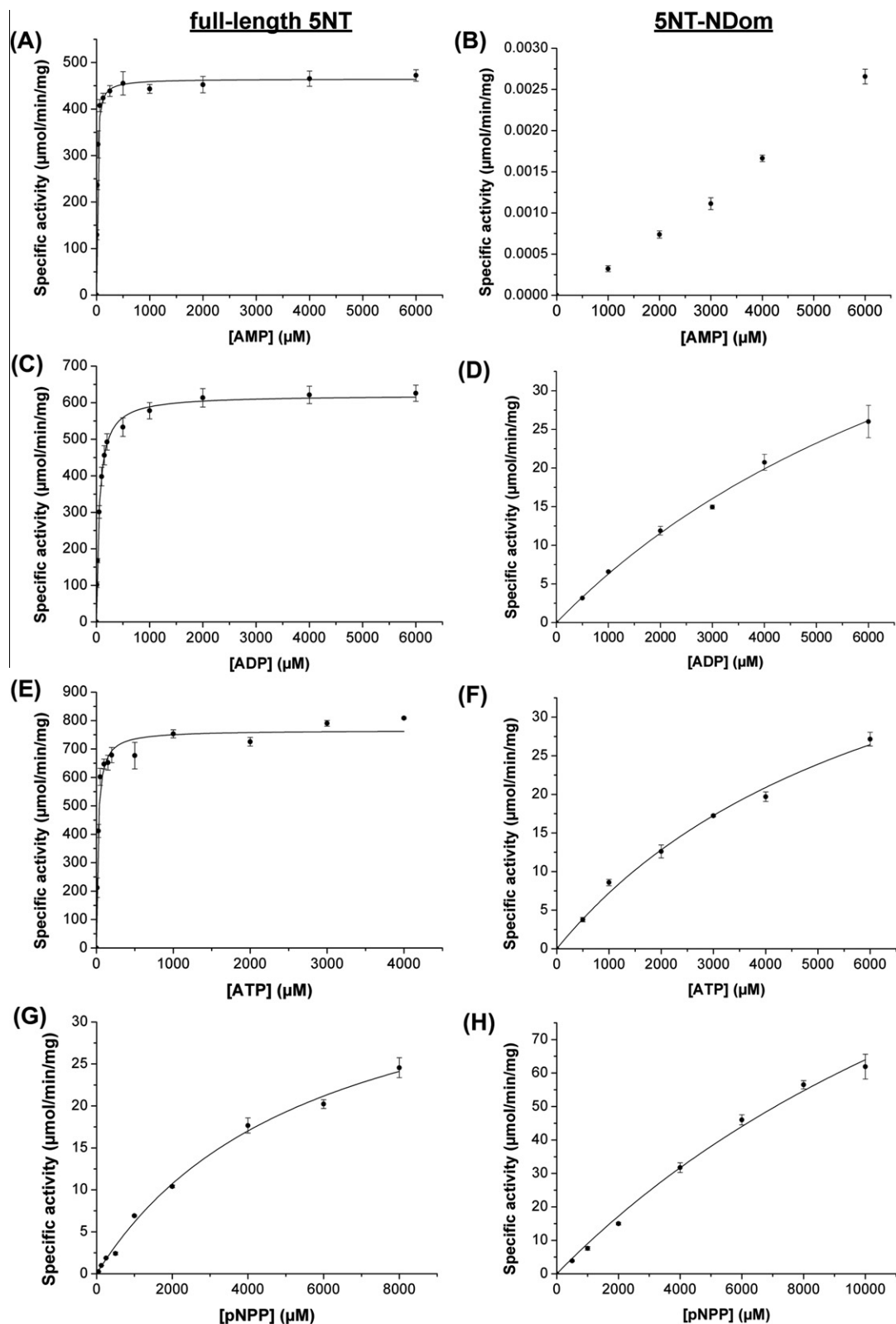


Fig. 4. Michaelis–Menten kinetics of the turnover of nucleotides and pNPP by full-length 5NT (A, C, E, G) and 5NT-NDom (B, D, F, H) in the presence of 5 mM CoCl_2 and 20 mM CaCl_2 .

3.2.2. Catalytic activity of the individual domains

5NT-NDom hydrolyzes adenine nucleotides as well as pNPP (Table 1, Fig. 4). For AMP only low turnover was observed.

Although it was not possible to fit the kinetic constants k_{cat} and K_m to the data, we estimated the specificity constant k_{cat}/K_m from the slope of the curve (Fig. 4B). It is reduced by a factor of about 10^8 compared to the reaction of full-length 5NT with AMP. With

45 and 36 s^{-1} , the turnover numbers of 5NT–NDom for ADP and ATP, respectively, are also decreased compared to the full length protein, but only by a factor of 13–20. These large differences in the cleavage of AMP compared to ADP and ATP by 5NT–NDom are likely to originate from the nature of the hydrolyzed bonds to the terminal phosphate group. The phosphoanhydride bonds in ADP and ATP are more labile than the ester bond cleaved in AMP. The phosphate groups of ADP and AMP are good (thermodynamically stable) leaving groups. In contrast, the alcoholate resulting from AMP cleavage is thermodynamically unstable and hence a weak leaving group. An activated phosphoester bond is also present in pNPP. The aromatic ring with the nitro group withdraws electrons from the O–P-bond and stabilizes the phenolic leaving group. Thereby, it facilitates the nucleophilic attack on the phosphate group and expulsion of the p-nitrophenolate. The k_{cat} of 5NT–NDom for pNPP is threefold higher than the k_{cat} for ADP and ATP (Table 1, Fig. 4).

Interestingly, the turnover of pNPP by 5NT–NDom is more than threefold higher in comparison to the full-length enzyme. This observation might be caused by a better accessibility of the active site cavity in 5NT–NDom. In full-length 5NT the presence of the C-terminal domain might hinder active site access for the small substrate, which does not require the C-terminal domain for binding.

For 5NT–CDom no hydrolysis of the nucleotides or pNPP was observed although Ca^{2+} and Co^{2+} were present in the assay buffer. The C-terminal domain alone is catalytically inactive due to the lack of the dimetal center and the Asp–His dyad. Binding of the three arginines R375, R379 and R410 to the phosphate groups of the substrates alone does not confer any measurable rate enhancement of the hydrolysis reaction.

Formation of the full-length protein in solution by mixing equimolar amounts of the two domains was neither observed in a native PAGE nor by any increase in the hydrolytic activity in the activity assays (data not shown). These findings indicate that the interactions between the two domains are too weak to reconstitute the full-length protein from the two folded individual domains without the presence of a covalent linker connecting both domains.

4. Discussion

4.1. Implications for the catalytic mechanism

The differences in the catalytic behavior of full-length 5NT and 5NT–NDom are related to the active site structure, which is formed at the domain interface (Fig. 1B). The adenine base and the ribose are bound by the C-terminal domain whereas the phosphate groups form contacts to N116, H117 and metal ion 2 of the N-terminal domain as well as R375, R379 and R410 from the C-terminal domain [4]. Assuming a similar binding mode of the terminal phosphate group to 5NT–NDom the interactions of the phosphate groups must be weakened compared to full-length 5NT as the arginines are not present to coordinate the phosphate groups and to provide electrostatic stabilization. An interesting result of the present study is that in contrast to earlier suggestions [4] the data determined for 5NT–NDom demonstrate that R375, R379 and R410 are not necessary for binding of the substrate phosphate groups or for transition state stabilization. This is indicated by the high catalytic turnover numbers of 5NT–NDom for ATP, ADP and pNPP. Based on the proposed mechanism [4], these results demonstrate that in 5NT–NDom H117 and the metal ions are sufficient for transition state stabilization of these substrates.

As mentioned in the previous section, the greatly reduced activity of the N-terminal domain to hydrolyze AMP (as opposed to ATP, ADP and pNPP) is likely due to the less activated ester bond and poor alcoholate leaving group in AMP. The coordination of the

phosphate group by the arginines of the C-terminal domain and/or the orientation of the AMP substrate for productive binding by the ribose and the adenine base binding pocket of the C-terminal domain are obviously essential for efficient hydrolysis of AMP.

For efficient expulsion of the leaving group, protonation of the instable alcoholate is necessary. In the assumed Michaelis complex based on the AMPCP cocrystal structure, there is no protein residue positioned to fulfill this role (Fig. 1B). The leaving group might be protonated by a water molecule. Alternatively, H117 might provide a proton, but it is 5.0 \AA away from the leaving group (in the AMPCP model). This distance might be smaller in the transition state complex. It is also possible that the AMPCP structure is no good model for the productive AMP binding mode. In any way, H117 is also present in 5NT–NDom and thus cannot explain the different reactivity of full-length 5NT and 5NT–NDom towards AMP.

As no structural data of 5NT–NDom in complex with a substrate are available up to now we can not rule out that new interactions are formed to stabilize the binding of the substrates. However, the kinetic data with K_{m} values in the mM range imply that these interactions would not be as strong as in full-length 5NT. In agreement with the suggestion that in full-length 5NT the artificial substrate pNPP does not bind to the C-terminal domain [7], the specificity constant of full-length 5NT for pNPP is comparable to those of 5NT–NDom for ATP and ADP.

4.2. Structure and function of the two 5NT domains in related proteins

5NT belongs to the calcineurin superfamily of phosphatases containing a dimetal center in the active site [5,16]. However, only the N-terminal domain is related to this protein superfamily. In some of these metallophosphatases, the N-terminal domain is catalytically active without the requirement of additional domains, e.g., in the mammalian purple acid phosphatases [17–20]. This demonstrates the ability of this domain to independently catalyze the hydrolysis of phosphoesters or anhydrides. The dinuclear metal ion center and the catalytic H117 are the conserved essential elements for catalysis [4].

The structure of the C-terminal domain is almost unique to the 5'-nucleotidases. A DALI search [21] for related domains revealed that the C-terminal domain is currently only found in the 5'-nucleotidases and the thiosulfohydrolase SoxB (alignment of 169 C α , rmsd of 2.4 \AA , PDB:2WDF). SoxB is an enzyme hydrolyzing a sulfur–sulfur bond. Both domains of SoxB are related to 5NT. Despite the similarities and the presence of a dimetal center, SoxB shows considerable differences. No domain motion was observed, the catalytic dyad is missing and the active site residues in the C-terminal domain are arranged differently [22]. As only the binding of the substrate analog thiosulfate is shown, not many interactions with the C-terminal domain are characterized. Nevertheless, it is very likely that similarly to 5NT the C-terminal domain is responsible for binding and positioning of the substrate and not for the core catalytic steps.

Furthermore, independent expression of the two domains provides an effective strategy for NMR signal assignment. The expression of each domain in a $^2\text{H}/^{13}\text{C}/^{15}\text{N}$ background is possible with a yield comparable to the ^{15}N -labeled protein (data not shown). The binding of AMPCP provided NMR spectra of comparable quality allowing structural and dynamic studies at residue resolution for the holo enzyme. This opens the way to NMR experiments to study the dynamics of the unique domain motion of the enzyme in solution.

In summary, our data show that catalysis in 5NT depends mainly on the N-terminal domain which is structurally related to a variety of other dinuclear metallophosphatases. On the other hand, the presence of the evolutionary not widely distributed C-terminal domain enhances the catalytic efficiency for non-activated substrates. It also provides the specificity for nucleotide

substrates by increasing the local concentration of the nucleotide substrates recognized by its specificity pocket. Thus, 5NT is an interesting example where the catalytic efficiency of an enzyme can be dissected to contributions from two evolutionary independent domains, one being predominantly responsible for the catalysis of the core chemical steps and the second for providing substrate specificity by binding the ribose and base moieties of the nucleotides.

The majority of the cross signals derived from the two domains could be superimposed on the signals given by full-length 5NT. For both domains more than 90% of the expected signals were observed likely enabling numerous assignments of the 60 kDa full-length 5NT protein with the individual sets of spectra.

Acknowledgments

We thank Susanne Moschütz for advice concerning the kinetic studies. Nicole Jahr and Stefan Berger are acknowledged for initial support with isotope-labeling of protein samples and NMR measurements. This work was supported by a grant of the Deutsche Forschungsgemeinschaft.

References

- [1] Neu, H.C. (1967) The 5'-nucleotidase of *Escherichia coli*. I. Purification and properties. *J. Biol. Chem.* 242, 3896–3904.
- [2] Ruiz, A., Hurtado, C., Meireles, R.J., Sillero, A. and Gunther Sillero, M.A. (1989) Hydrolysis of bis(5'-nucleosidyl) polyphosphates by *Escherichia coli* 5'-nucleotidase. *J. Bacteriol.* 171, 6703–6709.
- [3] Knofel, T. and Strater, N. (1999) X-ray structure of the *Escherichia coli* periplasmic 5'-nucleotidase containing a dimetal catalytic site. *Nat. Struct. Biol.* 6, 448–453.
- [4] Knofel, T. and Strater, N. (2001) Mechanism of hydrolysis of phosphate esters by the dimetal center of 5'-nucleotidase based on crystal structures. *J. Mol. Biol.* 309, 239–254.
- [5] Zimmermann, H., Zebisch, M. and Strater, N. (2012) Cellular function and molecular structure of ecto-nucleotidases. *Purinergic Signal.* 8, 437–502.
- [6] Knofel, T. and Strater, N. (2001) *E. coli* 5'-nucleotidase undergoes a hinge-bending domain rotation resembling a ball-and-socket motion. *J. Mol. Biol.* 309, 255–266.
- [7] Schultz-Heienbrok, R., Maier, T. and Strater, N. (2005) A large hinge bending domain rotation is necessary for the catalytic function of *Escherichia coli* 5'-nucleotidase. *Biochemistry* 44, 2244–2252.
- [8] Schultz-Heienbrok, R., Maier, T. and Strater, N. (2004) Trapping a 96 degrees domain rotation in two distinct conformations by engineered disulfide bridges. *Protein Sci.* 13, 1811–1822.
- [9] Hayward, S. (1999) Structural principles governing domain motions in proteins. *Protein Struct. Funct. Genet.* 36, 425–435.
- [10] Baykov, A.A., Evtushenko, O.A. and Avaeva, S.M. (1988) A malachite green procedure for orthophosphate determination and its use in alkaline phosphatase-based enzyme immunoassay. *Anal. Biochem.* 171, 266–270.
- [11] Zebisch, M. and Sträter, N. (2007) Characterization of Rat NTPDase1, -2, and -3 ectodomains refolded from bacterial inclusion bodies. *Biochemistry* 46, 11945–11956.
- [12] Delaglio, F., Grzesiek, S., Vuister, G.W., Zhu, G., Pfeifer, J. and Bax, A. (1995) NMRPipe: a multidimensional spectral processing system based on UNIX pipes. *J. Biomol. NMR* 6, 277–293.
- [13] Johnson, B.A. (2004) Using NMRView to visualize and analyze the NMR spectra of macromolecules. *Methods Mol. Biol.* 278, 313–352.
- [14] McMillen, L., Beacham, I.R. and Burns, D.M. (2003) Cobalt activation of *Escherichia coli* 5'-nucleotidase is due to zinc ion displacement at only one of two metal-ion-binding sites. *Biochem. J.* 372, 625–630.
- [15] Garcia, L., Chayet, L., Kettlun, A.M., Collados, L., Chiong, M., Traverso-Cori, A., Mancilla, M. and Valenzuela, M.A. (1997) Kinetic characteristics of nucleoside mono-, di- and triphosphatase activities of the periplasmic 5'-nucleotidase of *Escherichia coli*. *Comp. Biochem. Physiol. B: Biochem. Mol. Biol.* 117, 135–142.
- [16] Koonin, E.V. (1994) Conserved sequence pattern in a wide variety of phosphoesterases. *Protein Sci.* 3, 356–358.
- [17] Strater, N., Jasper, B., Scholte, M., Krebs, B., Duff, A.P., Langley, D.B., Han, R., Averill, B.A., Freeman, H.C. and Guss, J.M. (2005) Crystal structures of recombinant human purple acid phosphatase with and without an inhibitory conformation of the repression loop. *J. Mol. Biol.* 351, 233–246.
- [18] Uppenberg, J., Lindqvist, F., Svensson, C., Ek-Rylander, B. and Andersson, G. (1999) Crystal structure of a mammalian purple acid phosphatase. *J. Mol. Biol.* 290, 201–211.
- [19] Lindqvist, Y., Johansson, E., Kaija, H., Vihko, P. and Schneider, G. (1999) Three-dimensional structure of a mammalian purple acid phosphatase at 2.2 Å resolution with a mu-(hydr)oxo bridged di-iron center. *J. Mol. Biol.* 291, 135–147.
- [20] Guddat, L.W., McAlpine, A.S., Hume, D., Hamilton, S., de, J.J. and Martin, J.L. (1999) Crystal structure of mammalian purple acid phosphatase. *Structure* 7, 757–767.
- [21] Holm, L. and Rosenstrom, P. (2010) Dali server: conservation mapping in 3D. *Nucleic Acids Res.* 38, W545–W549.
- [22] Sauve, V., Roversi, P., Leath, K.J., Garman, E.F., Antrobus, R., Lea, S.M. and Berks, B.C. (2009) Mechanism for the hydrolysis of a sulfur–sulfur bond based on the crystal structure of the thiosulfohydrolase SoxB. *J. Biol. Chem.* 284, 21707–21718.